ISBN: 978-3-95450-208-0 doi:10.18429/JACoW-IPAC2019-WEPTS022

STABILITY TUNE DIAGRAM OF A HIGH-INTENSITY HADRON RING*

H. Okamoto†, Y. Tokashiki, K. Kojima, AdSM, Hiroshima University, Higashi-Hiroshima 739-8530, Japan

Abstract

To date, the optimum operating point of a high-intensity hadron ring has been determined on the basis of the conventional incoherent picture. It is generally chosen in the tune diagram such that the so-called "incoherent tune spread" of a stored beam does not overlap with low-order "single-particle resonance" lines. We here propose a new approach to construct the stability tune diagram on the basis of the self-consistent coherent picture. The betatron resonance condition recently conjectured from one-dimensional Vlasov predictions is employed for this purpose. The proposed general rule for the stability-chart construction is very simple and free from any model-dependent unobservables like space-charge-depressed incoherent tunes. As an example, we apply the present rule to the lattice of the rapid cycling synchrotron at J-PARC and explain why the operating bare tunes of this machine should be chosen slightly below 6.5 in both transverse directions.

INTRODUCTION

Resonance is inevitable in modern particle accelerators composed of a periodic array of identical alternating-gradient (AG) beam focusing lattices. The machine operating point has to be put sufficiently away from dangerous low-order resonance lines along which serious emittance growth and resultant beam loss may occur. The classical *single-particle resonance condition* given by Courant and Snyder can be written as

$$k\nu_{0x} + \ell\,\nu_{0y} = n, \tag{1}$$

where (ν_{0x}, ν_{0y}) are the horizontal and vertical *bare* betatron tunes per lattice period or around the ring, and (k, ℓ, n) are integers [1]. The driving term of this resonance is proportional to $x^{|k|}y^{|\ell|}$ whose order is $|k|+|\ell|(\equiv m)$.

Equation (1) has to be modified in high-intensity hadron machines and cooler storage rings where the space-charge interaction plays an important role. The natural repulsive force weakens the artificial focusing force from quadrupole magnets, leading to the reduction of effective betatron tunes down to $\nu_x(<\nu_{0x})$ and $\nu_y(<\nu_{0y})$ in both transverse directions. The magnitudes of the tune reduction, $\nu_{0x}-\nu_x$ $(\equiv \Delta\nu_x)$ and $\nu_{0y}-\nu_y(\equiv \Delta\nu_y)$, are referred to as *incoherent tune shifts*. The so-called *incoherent resonance condition* is obtained by simply replacing the bare tunes in Eq. (1) by the space-charge-depressed tunes, namely,

$$k\nu_x + \ell\,\nu_y = n. \tag{2}$$

The incoherent tune shifts take different values depending on which particle we observe. The effective tunes (ν_x, ν_y) of the particles forming a particular beam cover a finite area in the tune diagram, which is called the *incoherent tune spread*. As schematically illustrated in Fig. 1, we are required to choose the machine operating point P in the tune diagram such that the tune-spread area does not cross nearby low-order single-particle resonance lines predicted by Eq. (1). This type of stability chart has been often employed in the community to explain space-charge-induced beam loss in a high-intensity hadron machine or to decide the optimum operating point. The instability of the *beam core* in phase space is, however, expected to grow collectively rather than in an incoherent way, considering the reachable distance of the Coulomb interaction. In the present paper, we propose an alternative approach for the construction of a stability map in the betatron tune space, taking the collective nature of the core dynamics into account.

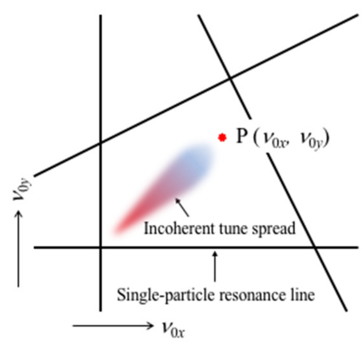

Figure 1: Conventional tune diagram based on the concept of incoherent tune spread.

COHERENT RESONANCES

Conventional Conditions

The first pioneering work on coherent resonances of a dense beam core was done by F. J. Sacherer who mathematically solved the one-dimensional (1D) Vlasov-Poisson equations using the uniform-density model [2]. Under the smooth approximation, he derived the resonance condition

$$m(\nu_0 - C_{mh}\Delta\nu) = n, \tag{3}$$

where ν_0 represents a transverse bare tune (either ν_{0x} or ν_{0y}), $\Delta\nu$ is the space-charge-induced tune shift in the corresponding direction, and C_{mh} is a constant factor with two indices representing the azimuthal (m) and radial (h) mode numbers. The Sacherer's analytic theory was extended by R. L. Gluckstern to a coasting round beam, i.e., the case where $\nu_{0x}=\nu_{0y}$ [3].

I. Hofmann *et al.* later proposed a two-dimensional (2D) coherent resonance condition, adding a correction term to Eq. (2):

$$k\nu_x + \ell\,\nu_y + \Delta\omega = n, \tag{4}$$

* Work supported in part by JSPS KAKENHI Grant Number 18H03472.
† okamoto@sci.hiroshima-u.ac.jp

ISBN: 978-3-95450-208-0 doi:10.18429/JACoW-IPAC2019-WEPTS022

where $\Delta\omega$ is the coherent tune shift away from the incoherent resonance condition [4]. The incoherent tunes in Eq. (4) have been defined assuming the uniform particle density. The coherent shift $\Delta\omega$ is a complicated function of several parameters. A few different values of C_{mh} are theoretically possible in the 2D case even for a specific order of mode with $m=h$ [5].

Betatron Resonance Ansatz

H. Okamoto and K. Yokoya (OY) generalized the Sacherer's approach, solving the 1D Vlasov-Poisson equations without the smooth approximation [6]. The OY theory predicts that the severe coherent resonance of the mth order may occur at high beam density under the condition

$$m(\nu_0 - C_m \Delta\bar{\nu}) = \frac{n'}{2}, \qquad (5)$$

where n' is an integer, the coherent tune-shift factor C_m depends only on the resonance order m, and $\Delta\bar{\nu}$ represents the root-mean-squared (rms) tune shift that can be related to the rms tune depression η as $\Delta\bar{\nu} = (1-\eta)\nu_0$. Particularly noteworthy is the factor 1/2 on the right-hand side that results in a two-fold increase of the density of resonances in the tune diagram. External imperfection fields can drive resonances only with even n'. The space-charge-driven resonances can take place regardless of the parity of n', but they are naturally weakened as the beam density decreases.

Since it is hopeless to solve the 2D Vlasov-Poisson equations mathematically for arbitrary AG lattices, a plausible conjecture was made recently in Ref. [7]. The proposed 2D resonance condition has a remarkably simple form, in spite of the complex collective process behind:

$$k(\nu_{0x} - C_m \Delta\bar{\nu}_x) + \ell(\nu_{0y} - C_m \Delta\bar{\nu}_y) = \frac{n'}{2}, \qquad (6)$$

where the horizontal and vertical rms tune shifts can be evaluated from $\Delta\bar{\nu}_{x(y)} = (1-\eta_{x(y)})\nu_{0x(0y)}$ with $\eta_{x(y)}$ being the rms tune depressions. Equation (6) is reduced exactly to Eq. (5) in the case of purely horizontal or vertical resonance where $(k,\ell) = (m,0)$ or $(0,m)$. In striking contrast with Eq. (4), Eq. (6) has the parametric factor 1/2 on the right-hand side and is free from any model-dependent unobservables, in other words, incoherent parameters. The rms tune shifts can uniquely be determined regardless of the form of the phase-space distribution function. Note also that the C_m-factor is constant over the whole tune space, unlike the coherent tune shift $\Delta\omega$ in Eq. (4) that depends on the integer numbers (k,ℓ), the beam ellipticity, and even the operating bare tunes [4,5].

COHERENT TUNE-SHIFT FACTORS

We performed a huge number of self-consistent simulations to estimate the C_m-factor, using the particle-in-cell code "WARP" [8]. Three-different types of initial particle distributions in phase space, i.e., Gaussian, waterbag, and parabolic, were adopted for this purpose. A typical distribution of resonance stop bands is shown in Fig. 2 where the emittance growth of the Gaussian beam after the transport over 100 AG periods is color-coded in the tune diagram. We have assumed the horizontal and vertical rms emittances to be equal at injection. The beam intensity and emittances are fixed over the whole tune space at specific values that give the tune depression of 0.9 at the operating point $(\nu_{0x}, \nu_{0y}) = (1/6, 1/6)$. The solid, dotted, and dashed lines in the picture are obtained from Eq. (6) with $C_m = 0$, 0.5, and 1.0, respectively, under the assumption that all visible emittance-growth bands are due to the linear $(m=2)$ and first nonlinear $(m=3)$ resonances. We see that each instability band is located roughly in-between the solid and dashed lines, which suggests that the C_m-factor is somewhat smaller than unity in these low-order modes. We tried several different initial conditions to figure out the parameter-dependence of these resonance stop bands [9]. Table 1 summarizes the results obtained by fitting the theoretical expectation from the coherent resonance formula to the positions of numerically observed non-coupling resonance bands. Similar tune-shift factors below unity have been found in the case of 2D coupling resonances as well.

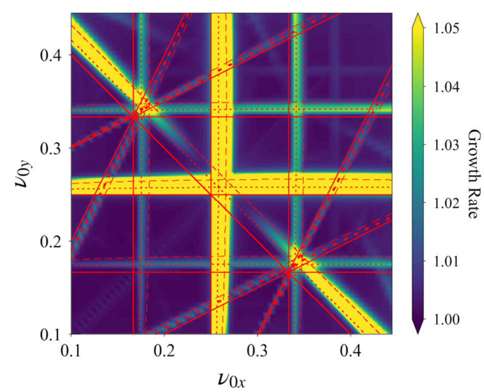

Figure 2: Stop-band distribution obtained from WARP simulations.

Table 1: Numerically Estimated C_m-Factors

	Gaussian	**Parabolic**	**Waterbag**
C_2	0.78 ± 0.05	0.73 ± 0.05	0.71 ± 0.04
C_3	0.77 ± 0.06	0.85 ± 0.04	0.87 ± 0.03
C_4	0.71 ± 0.06	0.87 ± 0.02	0.92 ± 0.01

SUPPRESSION OF DIFFERENCE RESONANCE BANDS

The difference resonance band along $k\nu_{0x} - k\nu_{0y} = 0$ is almost invisible in Fig. 2. This is because the horizontal and vertical rms emittances (ε_x, ε_y) have been set equal initially in these simulations, which deactivates the mechanism of emittance transfer under the condition $\nu_{0x} \approx \nu_{0y}$. Surprisingly, a similar simple argument can be made for arbitrary difference resonances, no matter whether the beam intensity is high or low. We have discovered that the difference resonances of a particular order can be eliminated by choosing the initial emittance ratio [9]

ISBN: 978-3-95450-208-0 doi:10.18429/JACoW-IPAC2019-WEPTS022

$$I_{k\ell} \equiv \frac{\varepsilon_x}{k} + \frac{\varepsilon_y}{\ell} = 0. \quad (7)$$

In the above-mentioned case where $k = -\ell$, Eq. (7) gives the magic emittance ratio $\varepsilon_x / \varepsilon_y = 1$ that has actually been fulfilled in Fig. 2 along $k\nu_{0x} - k\nu_{0y} = 0$.

Figure 3 shows another example where the horizontal emittance is set twice as large as the vertical ($\varepsilon_x / \varepsilon_y = 2$) everywhere in the tune space. The imperfection field proportional to $y^3 - 3x^2 y$ has been intentionally introduced to enhance the third-order resonances. Nevertheless, the difference resonance bands with $(k, \ell, n') = (2, -1, 0)$ and $(2, -1, 1)$ are invisible while the emittance growth has become very severe on the sum and vertical resonances of the third order. It is worth noting that the resonance band along $k\nu_{0x} - k\nu_{0y} = 0$ has now appeared clearly due to the breakdown of the condition $I_{k,-k} = 0$.

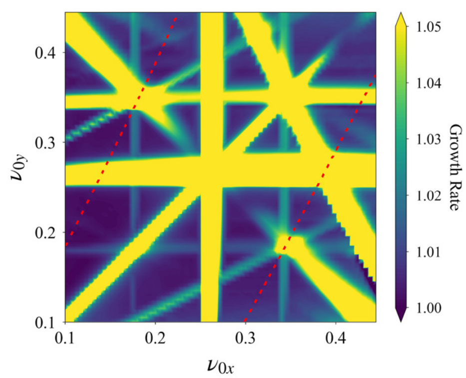

Figure 3: Stop-band distribution obtained from WARP simulations under the condition $\varepsilon_x / \varepsilon_y = 2$.

STABILITY MAP

The coherent resonance conjecture in Eq. (6) can be employed to provide a simple and practically useful guideline for the determination of the optimum machine operating condition. Our past experiences in ion-trap experiments and numerical simulations indicate that careful consideration to coherent resonances of up to the third order ($m \le 3$) is always demanded [7]. If the beam goes through a huge number of lattice periods before extraction or only very little emittance growth can be tolerated, we probably need to take care of the next order as well ($m \le 4$). Highly nonlinear modes are very weak and thus suppressed by the Landau damping mechanism unless strong nonlinear driving forces due to lattice imperfections are present in the machine.

On the other hand, it is extremely difficult to make a general quantitative argument on the band widths of coherent resonances. We here simply assume the widths of all stop bands to be equal to

$$\frac{\Delta\bar{\nu}}{\eta} \approx \frac{\lambda R r_{\rm p}}{4\varepsilon_\perp \beta^2 \gamma^3}, \quad (8)$$

where $r_{\rm p}$ is the classical particle radius, β and γ the Lorentz factors, λ the line density of the beam, R the average radius of the ring, and for simplicity we have put $\varepsilon_x \approx \varepsilon_y (\equiv \varepsilon_\perp)$ and $\eta_x \approx \eta_y (= \eta)$. This criterion will give us a sufficient safety margin because it has most likely overestimated the widths of nonlinear stop bands.

Let us apply the present rule to the lattice of the rapid cycling synchrotron (RCS) at J-PARC [10]. The RCS, whose circumference is $2\pi R = 348.333$ m, has a three-fold symmetric structure, which means that the driving harmonic numbers particularly important in practice are $|n'| =$ 0, 3, 6,… After the ideal injection painting at the kinetic energy of 400 MeV, the un-normalized edge emittance reaches 200πmm·mrad in both transverse directions. This corresponds to $\varepsilon_\perp \approx 50$ mm·mrad. The number of protons contained in a single bunch of 92 m long is about 4.165×10^{13}. Substitution of these numbers into Eq. (8) gives $\Delta\bar{\nu} / \eta \approx 0.13$.

Recalling the fitting results in Table 1, we assume that $C_2 = 0.75$ and $C_3 = 0.80$. The resultant distribution of the coherent resonance bands is sketched in Fig. 4 where all possible self-field-driven resonance bands of the second and third orders have been taken into account. The stop bands of the darkest shade can be enhanced by external imperfections. The narrow areas in-between a single-particle resonance line and its adjacent coherent stop band, indicated with a lighter shade, are potentially dangerous and thus should be avoided because a quasi-incoherent resonance may occur in the beam tail leading to non-negligible particle losses. The width of the difference resonance band along $k\nu_{0x} - k\nu_{0y} = 0$ has been disregarded in Fig. 4 because $\varepsilon_x \approx \varepsilon_y$ ($I_{k,-k} \approx 0$) in the RCS. After a careful tune survey, the operating point of the RCS has been chosen at around $(\nu_{0x}, \nu_{0y}) = (6.45, 6.42)$, which is perfectly consistent with the theoretical prediction in Fig. 4.

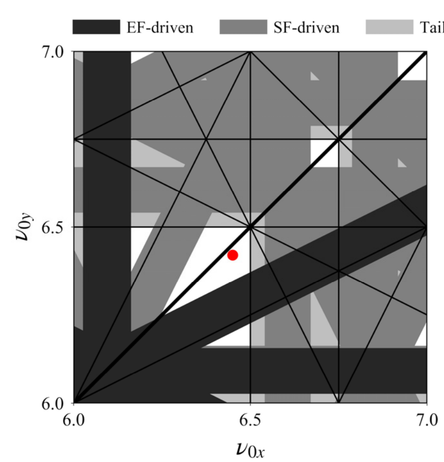

Figure 4: Tune diagram of the J-PARC RCS. The red dot indicates the optimum operating point of the RCS found through considerable experimental effort.

ISBN: 978-3-95450-208-0 doi:10.18429/JACoW-IPAC2019-WEPTS022

REFERENCES

[1] E. D. Courant and H. S. Snyder, "Theory of the alternating-gradient synchrotron", *Annals of Phys.*, vol. 3, pp. 1, 1958. doi:10.1016/0003-4916(58)90012-5

[2] F. J. Sacherer, "Transverse Space-Charge Effects in Circular Accelerators", Ph.D Thesis, Lawrence Radiation Laboratory, 1968.

[3] R. L. Gluckstern, "Oscillation Modes in Two Dimensional Beams", in *Proc. 1970 Linear Accelerator Conf. (LINAC'70)*, Batavia, IL, USA, Sep.-Oct. 1970, paper H-5, pp. 811-822.

[4] I. Hofmann *et al.*, "Space charge resonances in two and three dimensional anisotropic beams", *Phys. Rev. ST Accel. Beams,* vol. 6, pp. 024202, Feb 2003. doi:10.1103/PhysRevSTAB.6.024202

[5] R. Baartman, "Betatron resonances with space charge", in *AIP Conf. Proc*., vol. 448, pp. 56, May 1998. doi.org/10.1063/1.56781

[6] H. Okamoto and K. Yokoya, "Parametric resonances in intense one-dimensional beams propagating through a periodic focusing channel", *Nucl. Instr. Meth.*, vol. 482, pp. 51, Apr. 2002. doi.org/10.1016/S0168-9002(01)01684-9

[7] K. Ito *et al*., "Coherent resonance stop bands in alternating gradient beam transport", *Phys. Rev. Accel. Beams*, vol. 20, pp. 064201, Jun. 2017. doi:10.1103/PhysRevAccelBeams.20.064201

[8] D.P. Grote *et al.*, "Progress toward source-to-target simulation", *Nucl. Instrum. Meth.*, vol. 464, pp. 563, May 2001. doi.org/10.1016/S0168-9002(01)00142-5

[9] K. Kojima, H. Okamoto, and Y. Tokashiki, submitted for publication.

[10] H. Hotchi *et al.*, "Achievement of a low-loss 1-MW beam operation in the 3-GeV rapid cycling synchrotron of the Japan Proton Accelerator Research Complex", *Phys. Rev. Accel. Beams*, vol. 20, pp. 060402, Jun. 2017. doi:10.1103/PhysRevAccelBeams.20.060402